Progress in Organic Coatings 208 (2025) 109514

Contents lists available at ScienceDirect

Progress in Organic Coatings

journal homepage: www.elsevier.com/locate/porgcoat

Fluorine-free and breathable self-cleaning superhydrophobic CS/PDMS/PLA coatings on wearable cotton fabric with light-induced self-sterilization

Rutuja A. Ekunde [a,b], Rajaram S. Sutar [c], Sagar S. Ingole [a], Akshay R. Jundle [a], Pradip P. Gaikwad [a], Viswanathan S. Saji [d], Shanhu Liu [c], Appasaheb K. Bhosale [b,*], Sanjay S. Latthe [a,c,**]

[a] Self-cleaning Research Laboratory, Department of Physics, Vivekanand College (Autonomous), Affiliated to Shivaji University, Kolhapur 416003, India
[b] Self-cleaning Research Laboratory, Department of Physics, Raje Ramrao College, Affiliated to Shivaji University, Jath 416404, India
[c] College of Chemistry and Molecular Science, Henan University, Kaifeng 475004, People's Republic of China
[d] Interdisciplinary Research Center for Advanced Materials, King Fahd University of Petroleum & Minerals, Dhahran 31261, Saudi Arabia

ARTICLE INFO

Keywords:
Self-cleaning cotton
Superhydrophobic
Photothermal
Self-sterilizing
Antibacterial

ABSTRACT

Developing textiles with self-sterilization and self-cleaning properties for microbial deactivation in the medical sector and high-risk areas is becoming a hot research topic. Compared with traditional methods like chemical, UV irradiation, and heat sterilization for disinfection of microbials, photothermal self-sterilization combined with superhydrophobic self-cleaning has gained considerable attention. In this study, we have developed layered coatings of candle soot/polydimethylsiloxane (CS/PDMS) and polylactic acid (PLA) on cotton fabric to achieve photothermal self-sterilization and superhydrophobic self-cleaning properties. The CS nanoparticles generate heat when exposed to light, facilitating the photothermal effect. Meanwhile, the CS nanoparticles are integrated into the polymer network, creating a hierarchical rough structure that traps air and reduces the water contact area. PDMS is a vital binder for CS nanoparticles on cotton fabric, enhancing the durability of the composite layer and reducing surface energy. The photothermal and superhydrophobic effects of the developed coating successfully demonstrated self-sterilization and self-cleaning capabilities, respectively. The as-prepared coating exhibits high water repellence with a water contact angle of 159 ± 2° and a low sliding angle of 6°. Moreover, the surface temperature of coated cotton fabric rose to 70.2 °C within 60 s under 1 sun solar illumination. Furthermore, the coating demonstrated excellent mechanical stability by maintaining its superhydrophobicity even after 55 sandpaper abrasion cycles, 12 adhesive tape peeling cycles, 140 min of ultrasound and 90 min of washing treatment. Additionally, the coated cotton exhibited excellent flexibility, breathability, air permeability, water vapor transmission, self-sterilization against gram-positive *Staphylococcus aureus* and gram-negative *Pseudomonas aeruginosa* bacteria, and self-cleaning against dust contamination. The present results have high potential for developing advanced self-cleaning cotton fabrics with contactless sterilization of microbials for commercial applications.

1. Introduction

Ever-growing human health issues are caused by infections with several microbes and viruses through contact with the nose, eyes, mouth, and skin [1]. Viruses, bacteria, and other microbes can grow on the surfaces of protective equipment, including face masks, goggles, medical aprons, clothing worn daily in medical sectors and hazardous areas [2]. Recently, the outbreak of the coronavirus SARS-Cov-2 impacted the world in over 210 countries, infecting more than 20 million people and creating a global health emergency during 2020–2022 [1,3]. The World Health Organization (WHO) has recommended using face masks and personal protective equipment as an important mitigation strategy against the transmission of the respiratory virus [4–6]. Most face masks, aprons, and clothes are made from cotton

* Corresponding author.
** Correspondence to: S.S. Latthe, Self-cleaning Research Laboratory, Department of Physics, Vivekanand College (Autonomous), Affiliated to Shivaji University, Kolhapur 416003, India.
E-mail addresses: akbhosale1@gmail.com (A.K. Bhosale), latthes@gmail.com (S.S. Latthe).

https://doi.org/10.1016/j.porgcoat.2025.109514
Received 26 May 2025; Received in revised form 29 June 2025; Accepted 5 July 2025

fabric due to its flexibility, softness, smoothness, and breathability. However, on the surface of normal protective cotton-wearing equipment, viruses, bacteria, and other microbes can inevitably adsorb and grow, potentially infecting the human body [7]. Without disinfection, masks, aprons, and other wearable clothes discarded outdoors could spread diseases through airborne and water molecules. Hence, developing technologies to deactivate viruses, bacteria, and other microbes from cotton fabrics and reuse them is highly demanded.

Over the past several decades, various deactivation/sterilization methods have been developed to reduce the transmission of viruses, bacteria, and other microbes and prevent infections in the human body. Chemical and heat treatments are widely used to sterilize viruses and microbes. In chemical treatments, ethanol and hydrogen peroxide are recommended to deactivate viruses and microbials [8–10]. In heat treatment, boiling water or steam can be used for deactivation because viruses and microbes are unstable at temperatures above 70 °C [11,12]. However, chemical disinfectants, like alcohol and hydrogen peroxide, can be toxic if inhaled, ingested, or absorbed through the skin. It may also cause irritation to the skin on contact. They often require specific concentrations and conditions to be effective. Aerosolized disinfectants can lead to respiratory issues, and prolonged exposure may trigger allergic reactions and has been linked to cancer and hormone disruption [12]. If heat treatments are inadequate, pathogens may not be fully inactivated, endangering the health of those exposed. These treatments may demand more energy and time, particularly in large-scale operations, and also pose several health issues. To tackle these issues, a photothermal superhydrophobic coating has been developed, which facilitates contactless self-sterilization upon exposure to sunlight and exhibits superhydrophobic self-cleaning properties.

Recently, Zhong et al. [7] have developed a photothermal superhydrophobic coating by depositing a few layers of graphene onto a commercially available surgical mask, utilizing a unique dual-mode laser-induced forward transfer method, which resulted in outstanding self-cleaning and photothermal properties. Under the irradiation of sunlight (1 sun), the surface temperature of the mask quickly exceeds 80 °C, facilitating effective sterilization for reuse. The coating utilizes silver nanoparticles and graphene, enhancing pathogen deactivation through plasmonic heating and antimicrobial effects while adding photothermal absorption and superhydrophobicity to prevent droplet adherence. Kumar et al. [3] have fabricated a photoactive antiviral face mask, utilizing a dual-channel spray nanocoating of a hybrid of shellac/copper nanoparticles. The coating contains shellac, a natural hydrophobic biopolymer, enhancing water repellency and copper nanoparticles, which provide strong photothermal effects, antimicrobial and photocatalytic properties. The temperature of the photoactive mask rapidly increases to greater than 70 °C within 5 min, under solar illumination, which results in a high level of free radicals that disrupt the membrane of virus-like particles and make self-cleaning and reusable. The multi-walled carbon nanotubes (MWCNTs) and single-walled carbon nanotubes (SWCNTs) exhibit promising potential in photothermal conversion. Su et al. [13] developed a superhydrophobic CNT thin film using a vacuum-assisted layer-by-layer assembly method. This film exhibits impressive electrothermal and photothermal performance, with a water contact angle (WCA) of 165°. When voltage or light was applied to the MWCNT film, it generated heat of 60 °C within 60 s. Soni et al. [11] have introduced a single spray coating technique for the deposition of a superhydrophobic layer of SWCNTs on a melt-blown polypropylene (PP) surgical mask. Spraying SWCNTs creates a nanospike-like morphology on the PP surface, resulting in a coating with a WCA of 156.2° ± 1.8°. Under one sun illumination, the surface temperature of the PP surgical mask increases by more than 90 °C within 30 s, confirming its self-sterilization ability. Kumar et al. [12] have utilized molybdenum disulfide (MoS_2) nanosheets to modify polycotton due to its excellent antibacterial and photothermal phenomena. The surface temperature of MoS_2-modified polycotton increases by nearly 77 °C, making them ideal for sunlight-mediated self-disinfection. Pakdel et al. [14] have developed multifunctional photothermal superhydrophobic cotton fabric utilizing silver nanoparticles and polydimethylsiloxane (PDMS) by the dip-coating method. The coating exhibited a WCA of 171.31° along with the silver nanoparticles, enabling photothermal properties. The maximum temperature of the coating reached to 46.5°. Zhong et al. [15] have developed photothermal superhydrophobic surgical mask using a dual-mode laser-induced forward transfer process with additive deposition of laser-induced graphene. The temperature of the coated surgical mask elevates to over 80 °C within 100 s, under 1 sun irradiation, effectively sterilizing the virus. These studies support that photothermal superhydrophobic cotton fabrics are effective in realizing self-sterilizing and self-cleaning abilities, making them a promising material.

Besides, emerging photothermal materials such as MXenes [16] and perovskites [17] have been recognized for their high photothermal conversion efficiency. However, challenges such as the selection of photothermal components and complexity in the fabrication limit its practical application, hindering widespread adoption despite its remarkable properties. Candle soot (CS) is a cost-effective material that can be easily harvested from ordinary candles, requiring no complex synthesis processes [18]. In contrast, MXenes synthesis involves hazardous chemicals like hydrofluoric acid, and perovskites require precise synthesis with high-purity precursors, which add to their costs [19]. Generated through simple combustion, CS aligns with green chemistry principles and can be produced renewably from paraffin candles. It boasts a high light absorption rate of over 99 %, making it efficient for applications like photothermal use. While MXenes and perovskites also offer high conversion efficiency, their complexity and cost may not be justified for some uses. It can be easily integrated with other materials to enhance its properties and withstand high temperatures, unlike MXenes and perovskites, which have stability issues under heat and moisture. For resource-limited settings, CS offers a practical and functional alternative to sophisticated nanomaterials. Moreover, CS nanoparticles (CS NPs) are generally considered to be low in toxicity to human skin. CS is biodegradable. In contrast, MXenes can degrade in air and moisture, potentially releasing toxic metal ions such as vanadium, raising concerns about their environmental impact [20]. Lead-based perovskites are unstable and can release toxic lead ions over time, posing ecological risks.

In this study, we developed a photothermal superhydrophobic coating on cotton fabric using a composite of CS and PDMS, applied through a simple and cost-effective dip-coating method. The CS NPs provided the required photothermal effect, generating the heat energy necessary for self-sterilization. PDMS, known for its low surface energy, also served as a binder, effectively connecting the CS NPs to the cotton surface and creating a micro-nano hierarchical surface structure. Additionally, polylactic acid (PLA) was incorporated to enhance the bonding strength between the cotton surface and the CS/PDMS composite. Although CS [21–23], PDMS [14,24–26] and PLA [27,28] were used in several recent reports on superhydrophobic cotton fabrics, this work uniquely combines them to yield an optimized coating, yielding highly durable superhydrophobic cotton fabrics with photothermal conversion efficiency. Experimental results demonstrated that the surface temperature of the coating rose to 70.2 °C within just 60 s of 1 kW/m^2 light exposure. The micro-nanostructure composed of CS NPs, PLA, and PDMS imparts superhydrophobicity to the surface, achieving a WCA of 159°. These synergistic properties of photothermal and superhydrophobicity of modified coated cotton fabric significantly disinfect bacterial contamination. Thus, the dual functionality of cotton fabric may have impactful commercial applications in healthcare, apparel, public safety, and industrial sectors.

2. Experimental section

2.1. Materials

Cotton fabric (mass density- 0.47 g/cm^3, air permeability-168 mm s^{-1} and thickness- 0.13 mm) was obtained from DKTE Textile Industry,

Maharashtra, India. Polydimethylsiloxane (PDMS, viscosity 5 cSt) was procured from Sigma-Aldrich, India. Chloroform (99 % AR) was bought from Spectrochem Pvt. Ltd., India. Polylactic acid (PLA, Mw ~ 80,000 g/mol and particle size of 3 mm) was purchased from Macklin (Shanghai, China). Candles were purchased from the local market. Candles were utilized to synthesize candle soot.

2.2. Synthesis of candle soot nanoparticles

Initially, soot layers were collected onto a metal plate by moving it within the central region of a candle flame. The accumulated soot was subsequently scraped off and stored in a glass container. A 500 mg of the collected soot was dispersed in 100 mL of chloroform and subjected to ultrasonication for 20 min, facilitating the disaggregation of the layered soot into finer particles. The mixture was then filtered through a 25 μm stainless steel mesh to isolate uniform soot particles. The resulting dispersion was then dried on a hot plate at 40 °C to ensure the complete evaporation of the chloroform. Once the solvent was entirely removed, the dried residue was finely crushed using a mortar and pestle to produce homogeneous soot particles, which were subsequently stored in a glass bottle for further experimental use.

2.3. Fabrication of photothermal superhydrophobic cotton

The fabrication of multifunctional cotton fabrics involves applying layers of PLA and CS/PDMS on pre-cleaned cotton. Cotton fabrics cut into 3 cm × 3 cm pieces were ultrasonically cleaned with ethanol and distilled water for 15 min each and then dried in an oven at 60 °C for 30 min to remove surface impurities. The cleaning process could help enhance the coating adhesion. A 0.024 g of PLA was dissolved in 25 mL of chloroform and stirred at 450 rpm for 1 h to produce solution A. Concurrently, in a separate beaker, solution B was prepared by adding 2 mL of PDMS in 25 mL of chloroform and stirred at 450 rpm for 30 min. Subsequently, 350 mg of CS NPs were incorporated and stirred for an additional 30 min to achieve a consistent dispersion. The cleaned cotton piece was first soaked in solution A for 5 min and air-dried for 1 min at room temperature. It was then soaked in solution B for another 5 min and air-dried for 1 min at room temperature. This entire process constituted one cycle. To optimize coating, the cotton samples underwent multiple coating cycles such as 5, 7, and 9, and were finally dried at 120 °C for 2 h. The resulting samples were labelled CP-1, CP-2, and CP-3, respectively. The synthesis of photothermal superhydrophobic coating on the cotton fabric is schematically shown in Fig. 1.

2.4. Characterization

The surface morphology and elemental composition of the coated cotton fabric samples were examined by using Field Emission Scanning Electron Microscopy (FESEM) (JEOL, JSM-7610F, Japan), coupled with energy-dispersive X-ray spectroscopy (EDS). A Stylus profiler (Mitutoyo, SJ-210, Japan) was used to evaluate the surface roughness of the samples. The elemental composition and chemical state of coatings were studied by X-ray Photoelectron Spectroscopy (XPS) (Thermo Fisher Scientific, Escalab 250Xi, USA). The chemical bonding of the coating was examined using Fourier Transform Infrared Spectroscopy (FT-IR) (Bruker, Germany, VERTEX 70). The absorption in the 200–2500 nm was measured using an UV–visible near-infrared spectrophotometer (Agilent, TY2021006984, China). A contact angle meter (HO-IAD-CAM, Holmarc Opto-Mechatronics, India) was used to determine the coating's water contact angle (WCA) and sliding angle (SA). A digital thickness tester (SDL ATLAS K094) was used to measure the thickness of the sample according to ASTM D1777. The average particle size of CS NPs was determined by ImageJ software.

A mechanical testing machine (Instron 5565, USA and Canada) was employed to measure the tensile strength of both pristine and coated cotton fabrics. An infrared thermal imager (FLIR, E8, USA) was used to measure the surface temperature of the samples. At the same time, irradiation intensity was adjusted using an irradiance meter (Perfect Light, PL-MW2000, China). A Testex air permeability tester was employed to determine air permeability at room temperature at a pressure of 100 Pa. The breathability of samples was investigated through an ammonia-hydrochloric acid reaction [30].

2.4.1. Self-cleaning test

Self-cleaning is one of the most remarkable properties of superhydrophobic surfaces. The self-cleaning tests were carried out on both pristine and coated cotton fabrics. The pristine and coated cotton fabrics were pasted onto the glass substrate utilizing a double-sided tape and inclined into a petri dish. Contaminants such as soil particles and chalk powder were randomly sprinkled onto the surface to simulate real-world dirt deposition. The water droplets were subsequently introduced on the surface to study self-cleaning performance.

2.4.2. Antibacterial test

The antibacterial activity of pristine and coated fabrics was thoroughly investigated against *Staphylococcus aureus* (NCIM 5345) and *Pseudomonas aeruginosa* (9027) using the agar disk diffusion method. To initiate this process, a suspension of the pathogens was precisely prepared in sterile saline to ensure optimal conditions for subsequent testing. For the antimicrobial activity assessments, the pathogens were evenly inoculated onto the surface of sterile Mueller-Hinton agar plates, a standard medium for antibiotic susceptibility testing. A sterile spreader was employed to ensure a uniform distribution of the inoculum across the agar surface.

Fabric samples of size 1 cm × 1 cm were first sterilized by exposure to ultraviolet (UV) light for 15 min. This process effectively neutralized

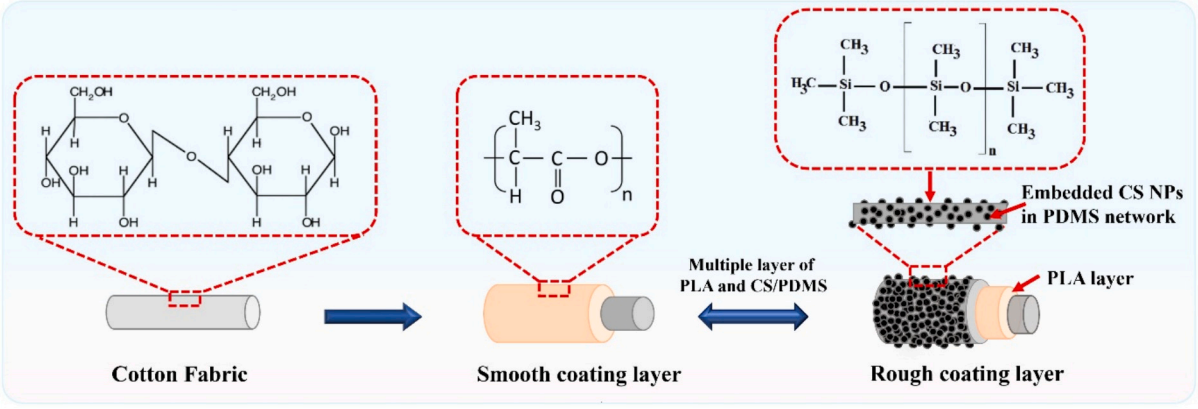

Fig. 1. Schematic illustration of the fabrication of photothermal superhydrophobic cotton fabric.

microorganisms, ensuring the samples were safe for testing and preserving the integrity of the results. Once sterilized, the fabric samples were aseptically placed on the surface of the agar plates that had previously been inoculated with the test pathogens. To evaluate the antibacterial effects, the plates were exposed to a near-infrared (NIR) laser at a wavelength of 700 nm for 10 min. This exposure assessed whether the coated fabrics possess any inherent photothermal antibacterial properties.

The plate count method was used to evaluate the effectiveness of fabrics against the bacteria. A 100 μL bacterial suspension was inoculated into 10 mL of sterile Mueller-Hinton broth and incubated at 37 °C until it reached an optical density of 0.6–0.8. Then, 100 μL of this suspension was transferred into test tubes with 9 mL of broth, and sterilized fabric samples were added. These were placed in a rotary shaker at 37 °C for 10 min. Samples (10 μL) were taken out at 5 and 10 min and spread onto sterile Mueller-Hinton agar plates. After incubating the plates at 37 °C for 24 h, visible colonies were counted as colony-forming units (CFUs) using the following formula [12].

$$\text{Bacterial survival}\ (\%) = \frac{\text{No of colonies on test sample}}{\text{No of colonies on control sample}} \times 100 \quad (1)$$

3. Results and discussion

3.1. Surface and chemical properties

The cotton fabric is first immersed in the PLA solution, forming a uniform layer that enhances structural integrity and functionality. Subsequently, the CS/PDMS coating is applied using a similar dip-coating method, which provides a strong bond to the PLA layer, along with additional biocompatibility, waterproofing, and flexibility characteristics. For optimization, multiple PLA and CS/PDMS layers were applied to cotton fabric. Cotton fibers, which are abundant in hydroxyl groups, form strong hydrogen bonds with PLA. This chemical interaction significantly enhances the adhesion between PLA and cotton fabric, leading to improved structural integrity. Additionally, the interface between the PLA-coated cotton fabric and the CS/PDMS composite layer relies on physical interactions that ensure strong adhesion of coating materials. CS NPs are primarily composed of hydrophobic polyaromatic hydrocarbons, which have low polarity [31]. Furthermore, the PDMS acts as binding agent as well as a low surface energy materials. The hydrophobic CS NPs interact with the non-polar PDMS through van der Waals forces, mainly driven by dispersion forces [29]. The combination of these diverse interactions between the CS NPs and PDMS creates a strong adhesion, resulting in a reliable interface that enhances the overall properties of the composite material. This multi-faceted bonding approach highlights the complexity and effectiveness of integrating these materials for improved performance. The chemical structures of cotton fabric, PLA, and PDMS are provided in Fig. 1. Fig. 2 illustrates the expected multifunctional properties of the developed surface: superhydrophobic self-cleaning and photothermal self-sterilization.

Fig. 3a, e and i illustrate the SEM images of the original cotton fabric, which presented a relatively smooth microstructure, characterized by unaltered fibers and uniform texture. The deposition of the CS/PDMS/PLA composite layer onto cotton fabric significantly enhances adhesion between the fibers. This interaction transforms the fabric's surface topography, adding texture and complexity to what was once a smooth finish. The aggregation of CS NPs contributes to developing a rough texture atop the initially smooth cotton surface. Fig. S1 illustrates the morphology of the synthesized CS NPs, which are approximately spherical and measure around 46.22 ± 7.6 nm in diameter. Their network-like structure is formed through weak Van der Waals forces. The SEM images of the CP-1 sample reveal that five layers of the CS/PDMS and PLA composite layers create a uniform coating on the cotton fabric, while maintaining its structure and preserving its micropores, which are essential for breathability and moisture-wicking. Figs. 3b, f and j illustrate the strong bond between the composite layers and the cotton fibers. The coating surface roughness is 11.40 μm (Fig. 3p). The retention of porosity is crucial for cotton's suitability in wearable applications across various sectors, as these properties ensure comfort and breathability. In contrast, when a greater number of layers, specifically seven layers of the CS/PDMS and PLA composite (designated as CP-2), were deposited on the cotton fabric, it became apparent that while a cohesive composite coating was formed, there was also a notable aggregation of composite materials. This aggregation appeared to be randomly distributed over the coating, as depicted in Figs. 3c, g and k. The micro-aggregation of the composite materials resulted in a hierarchical rough structure on the cotton surface, with a surface roughness of 14.51 μm (Fig. 3q). Such coating revealed a thickness of 0.02 mm (see Supplementary Information). However, with a further increase in the number of CS/PDMS and PLA layers, the SEM image revealed a lack of

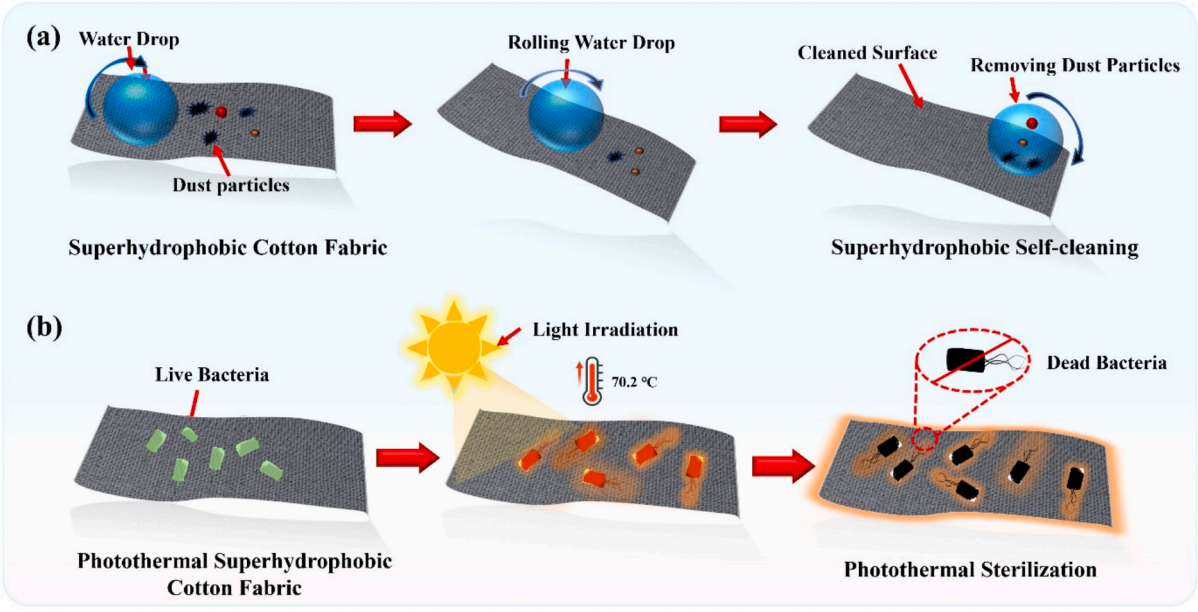

Fig. 2. Schematic illustration of (a) superhydrophobic self-cleaning, and (b) photothermal effect and self-sterilization under NIR light radiation.

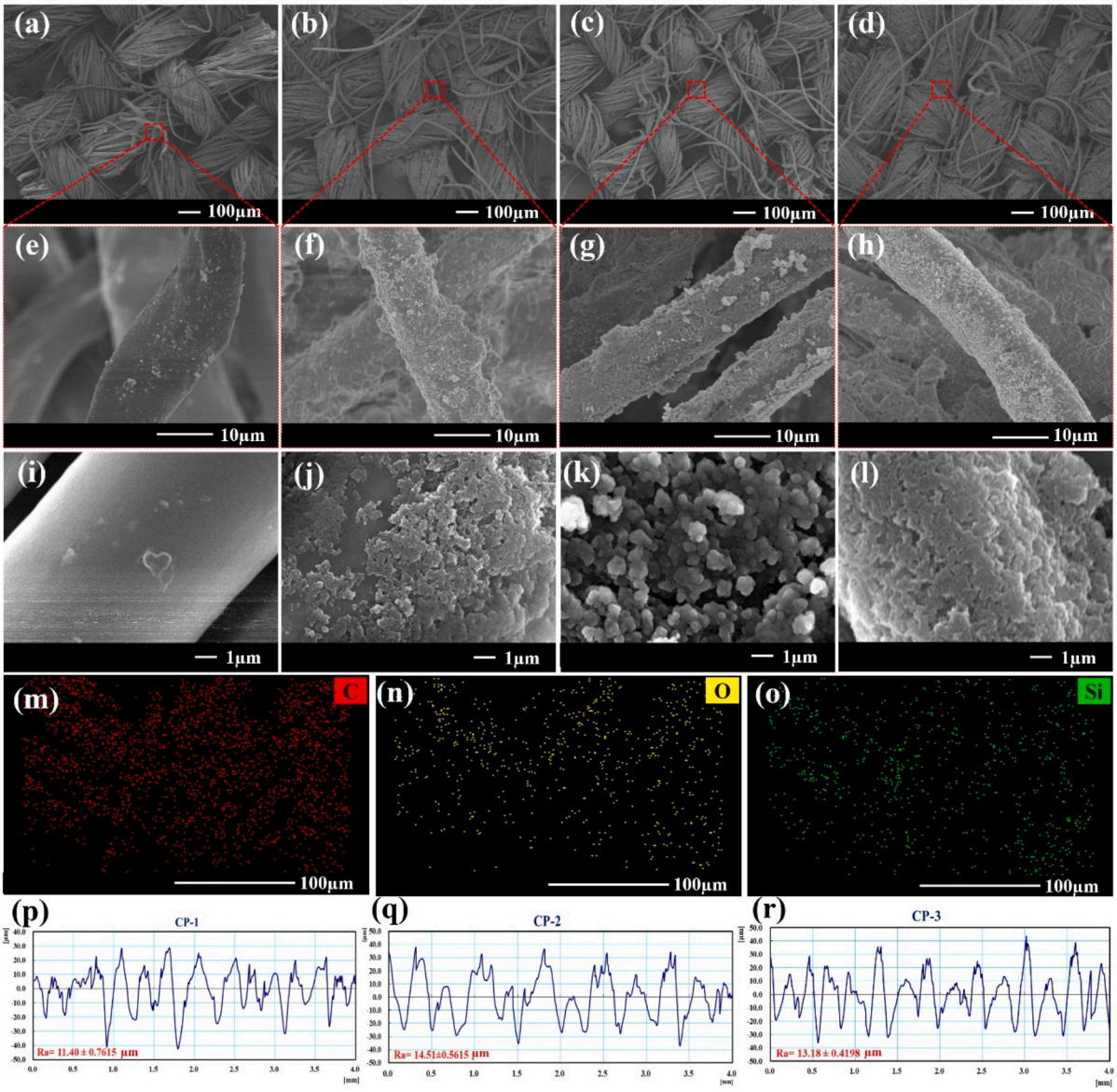

Fig. 3. SEM images of (a, e and i) pristine cotton, (b, f and j) CP-1, (c, g and k) CP-2 and (d, h and l) CP-3 samples. (m-o) EDS elemental mappings images of CP-2 sample. (p-r) Surface roughness of CP-1, CP-2, and CP-3 samples.

visible aggregated composite material as shown in Fig. 3d and h. The surface roughness of CP-3 slightly reduces to 13.18 μm (Fig. 3r). The EDS elemental investigation detected three major elements C, O and Si and their mapping images are shown in Fig. 3m-o. The majority of element C is attributed to CS [18], while Si corresponds to PDMS [32].

The chemical structure of the coated fabric was investigated through FT-IR and XPS analysis. In the FT-IR spectrum of pristine cotton, a prominent peak in the range of 2800–3300 cm^{-1} corresponds to the stretching vibrations of the hydroxyl (-OH) groups inherent to the cellulose structure. Additionally, a minor peak at 1650 cm^{-1} is associated with the O—H bending vibrations of adsorbed water, while the peak at 1065 cm^{-1} is indicative of C-O-C stretching due to cellulose structure (Fig. 4a). The FT-IR spectrum of only PLA-coated cotton reveals characteristic peaks at 1720 cm^{-1}, 1083 cm^{-1}, and 714 cm^{-1}, corresponding to the carbonyl (C=O), carbon-oxygen (C—O), and carbon-hydrogen (C—H) moieties, respectively (Fig. S2). For only PDMS-coated cotton fabric, an absorption peak at 2962 cm^{-1} indicates the asymmetric stretching of C—H bonds in the -CH_3 group, while additional peaks at 793 cm^{-1} and 1260 cm^{-1} are attributed to -CH_3 rocking and Si—C stretching in Si-CH_3 groups. The antisymmetric and symmetric vibrational peaks at 1022 cm^{-1} and 1086 cm^{-1} further confirm the presence of Si-O-Si functionalities within the PDMS structure (Fig. S2) [33]. As a result, the FT-IR spectra of the CS/PDMS and PLA layer coated cotton fabric (Fig. 4a) demonstrate significant absorption peaks reflecting various molecular vibrations. The peak at 2923 cm^{-1} is attributed to asymmetric C—H stretching in the methyl (-CH_3) groups [25]. A peak at 1238 cm^{-1} relates to vibrational modes of Si-CH_3 groups, confirming the incorporation of organosilicon components. Peaks within the range of 800 cm^{-1} to 470 cm^{-1} illustrate contributions from silicon moieties, while the peak at 1067 cm^{-1} indicates Si-O-Si bond vibrations typical of siloxane structures [34]. Finally, the peak at 682 cm^{-1} represents Si—C bond vibrations in dimethyl siloxane (Si-$(CH_3)_2$), underscoring the substantial presence of PDMS in the coatings [34–36].

The XPS analysis of the optimized coating CP-2 reveals three major peaks at binding energies of 103 eV, 285 eV, and 533 eV, corresponding to Si2p, C1s, and O1s signals (Fig. 4b) [37]. This indicates the presence of candle soot particles along with PDMS and PLA in the coating. The deconvoluted C1s spectrum shows three types of carbon bonding at 284.8 eV (C-C/C-H), 286.4 eV (C—O), and 289 eV (C=O) (Fig. 4c) [38]. Additionally, the Si 2p spectrum displays peaks at 102.32 eV and 103.7

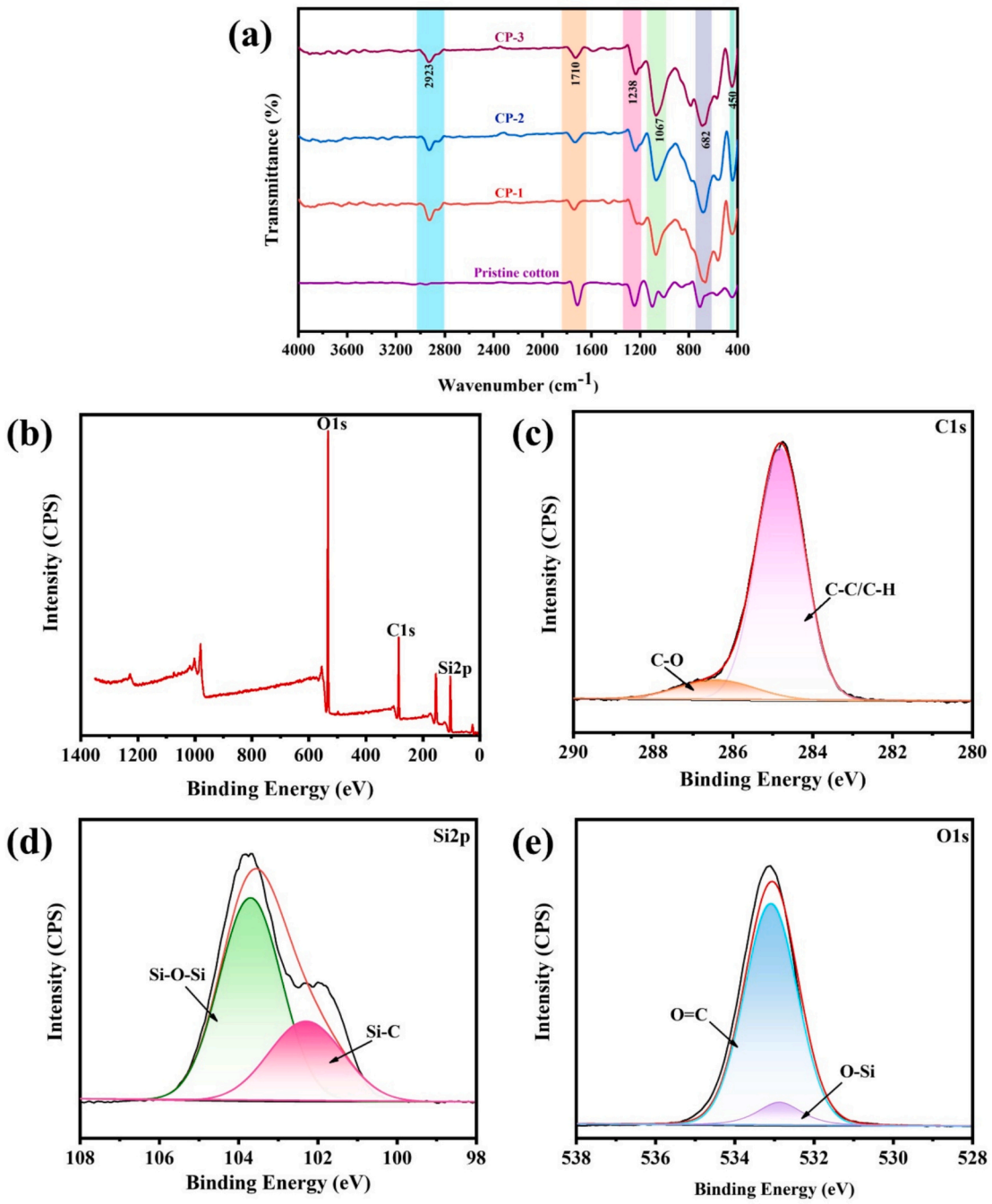

Fig. 4. (a) FT-IR spectra of pristine and coated cotton fabrics. (b) XPS full spectrum and high-resolution spectra of CP-2 sample (c) C1s, (d) Si2p, and (e) O1s scans.

eV, attributed to Si—C and Si-O-Si bonding (Fig. 4d) [39]. The O1s spectrum features two peaks linked to C═O and O—Si bonding, highlighting silicon-oxygen interactions (Fig. 4e). The FT-IR and XPS analysis confirms the chemical composition and interactions within the coating matrix.

3.2. Wettability and photothermal effect

Due to the presence of many hydroxyl groups, the pristine cotton exhibited a hydrophilic nature, which rapidly absorbs water, as illustrated in Fig. 5a. However, a significant transformation occurred after applying the composite coating, yielding superhydrophobicity. The CP-1 sample demonstrated a WCA of 151°, indicating effective water repellency. The CP-2 sample demonstrated an even higher WCA of 159°, which suggests improved superhydrophobic properties. However, the CP-3 sample exhibited a slight decrease in WCA (153°). This reduction can be attributed to the formation of a smoother surface texture. The CP-2 coating achieved the highest WCA of 159°, indicating high water repellence. The increase of WCA with the rise in the number of layered coatings is linked to the increasing surface roughness of the fabrics, which, in synergy with the low surface energy properties of PDMS, contributed to effective superhydrophobicity. However, increasing the number of coating layers beyond an optimal point led to a decline in WCA values due to the smoothing of the fiber surface, reducing micro-scale roughness. This loss in texture diminishes the surface's ability to trap air.

The efficacy of the coatings was further demonstrated in practical applications, where the coated fabrics displayed strong repellence

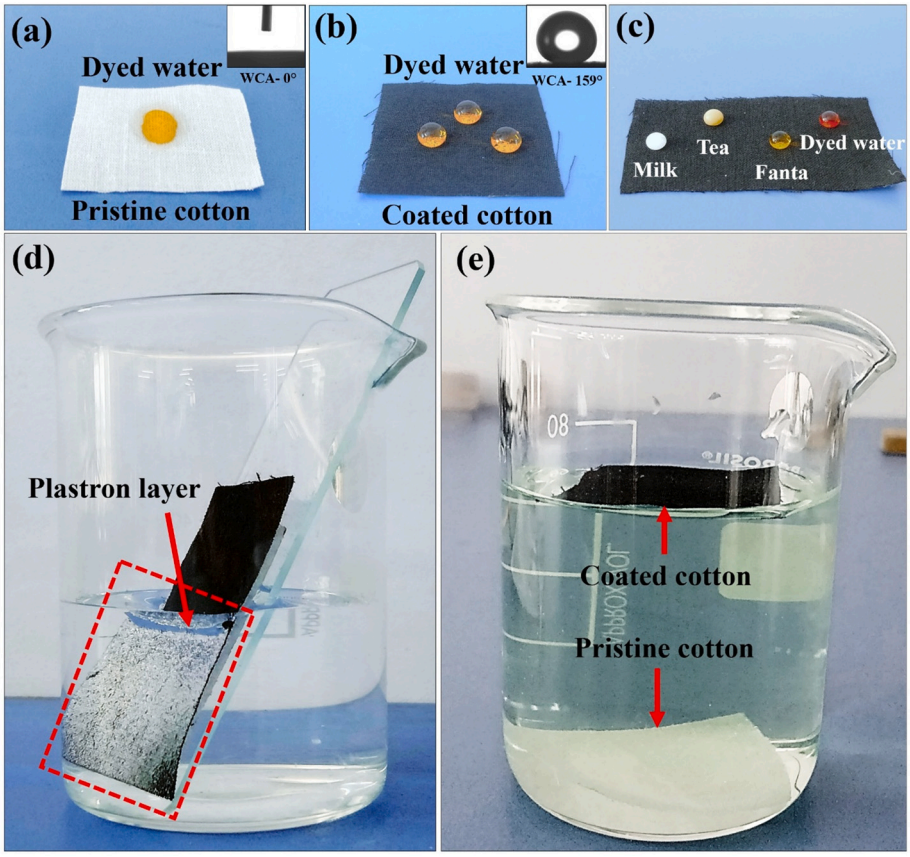

Fig. 5. Orange dyed water on (a) pristine cotton and (b) coated (CP-2) cotton fabrics; WCA image in inset, (c) Milk, Tea, Fanta, and red dyed water drop on CP-2 sample, (d) Mirror-like phenomena on CP-2 sample dipped in water, (e) Pristine and coated (CP-2) samples freely placed into colored water. (For interpretation of the references to colour in this figure legend, the reader is referred to the web version of this article.)

against various common types of water-based stains, including milk, tea, soft drink (Fanta), and dyed water stains, as shown in Fig. 5c. Remarkably, a mirror-like finish was observed on the superhydrophobic cotton fabric (CP-2) post-immersion in water, indicative of the successful formation of an air layer on the fabric's surface, as highlighted in Figs. 5d-e. Additionally, the CP-2 sample was measured to have a low SA of 6°. Such a feature is advantageous for maintaining the cleanliness of the fabric surface. Notably, when these samples were freely placed in water, the coated cotton displayed buoyancy, floating on the water's surface. In contrast, the untreated cotton sank immediately, as depicted in Fig. 5e, further underscoring the superior hydrophobicity imparted by the multilayered coatings.

The surface energy of the CP-2 sample was calculated using Eq. (2) [40],

$$W_{SL} = \gamma_{LA}(1 + cos\ \theta_o) \quad (2)$$

Here, θ_o is the static contact angle, W_{SL} is the work of adhesion per unit area between two surfaces and γ_{LA} is the surface energy (surface tension) of the liquid against air. The calculated surface energy for CP-2 sample was 4.7808 mN/m, significantly lower than that of pristine cotton (144 mN/m). This notable reduction indicates the formation of a lower-energy surface. To access the wetting behaviour, the solid-liquid contact fraction (f) was determined by the Cassie-Baxter model, as shown in Eq. (3) [41],

$$\text{Cos}\ \theta_{CB} = \text{f}\ (\text{Cos}\theta_0 + 1) \quad (3)$$

The solid-liquid fraction of the CP-2 sample is calculated to be 0.03015.

The light absorbance capabilities of the CP-2 sample in comparison to pristine cotton were analysed using UV–vis-NIR spectroscopy (Fig. 6a). Pristine cotton demonstrates a significantly limited capacity for light absorption, indicating its overall ineffective performance. In contrast, the CP-2 sample exhibits a notably enhanced light absorbance across the broad wavelength range of 250 to 2500 nm [42]. This significant light absorption in the ultraviolet, visible, and NIR regions is crucial, as it correlates with heat energy generation through the photothermal effect, which can be utilized for self-sterilization. These enhanced characteristics can be attributed to the integration of CS NPs within a PDMS matrix, coupled with the development of a hierarchical rough structure on the cotton fibers. The hierarchical structure of superhydrophobic coatings is beneficial to trap light through internal reflections, which improves light absorption efficiency [23]. Carbon-based CS NPs exhibit excellent light absorption and efficiently convert light energy into heat through lattice vibrations. When exposed to low-energy light, the π electrons in their frameworks undergo transitions from a lower energy level to a higher one (π*), enhancing their light-harvesting properties across UV, visible, and NIR wavelengths. The absorbed light energy is quickly converted into thermal energy, leading to localized heating on the coating's surface [43]. This rapid energy dissipation enhances the photothermal response, making these coatings ideal for applications in light-induced self-sterilization, promoting surface cleanliness, and facilitating the development of self-cleaning materials in various environments. Fig. S3 shows the schematic of the photothermal conversion of photothermal superhydrophobic cotton fabric.

The photothermal characteristics of uncoated and coated cotton samples were evaluated under a xenon lamp emitting 1 kW/cm^2 light intensity. Prior studies have demonstrated that CS NPs exhibit distinct photothermal effects, which have been utilized across diverse applications, including thermoregulating textiles [44], artificial muscle

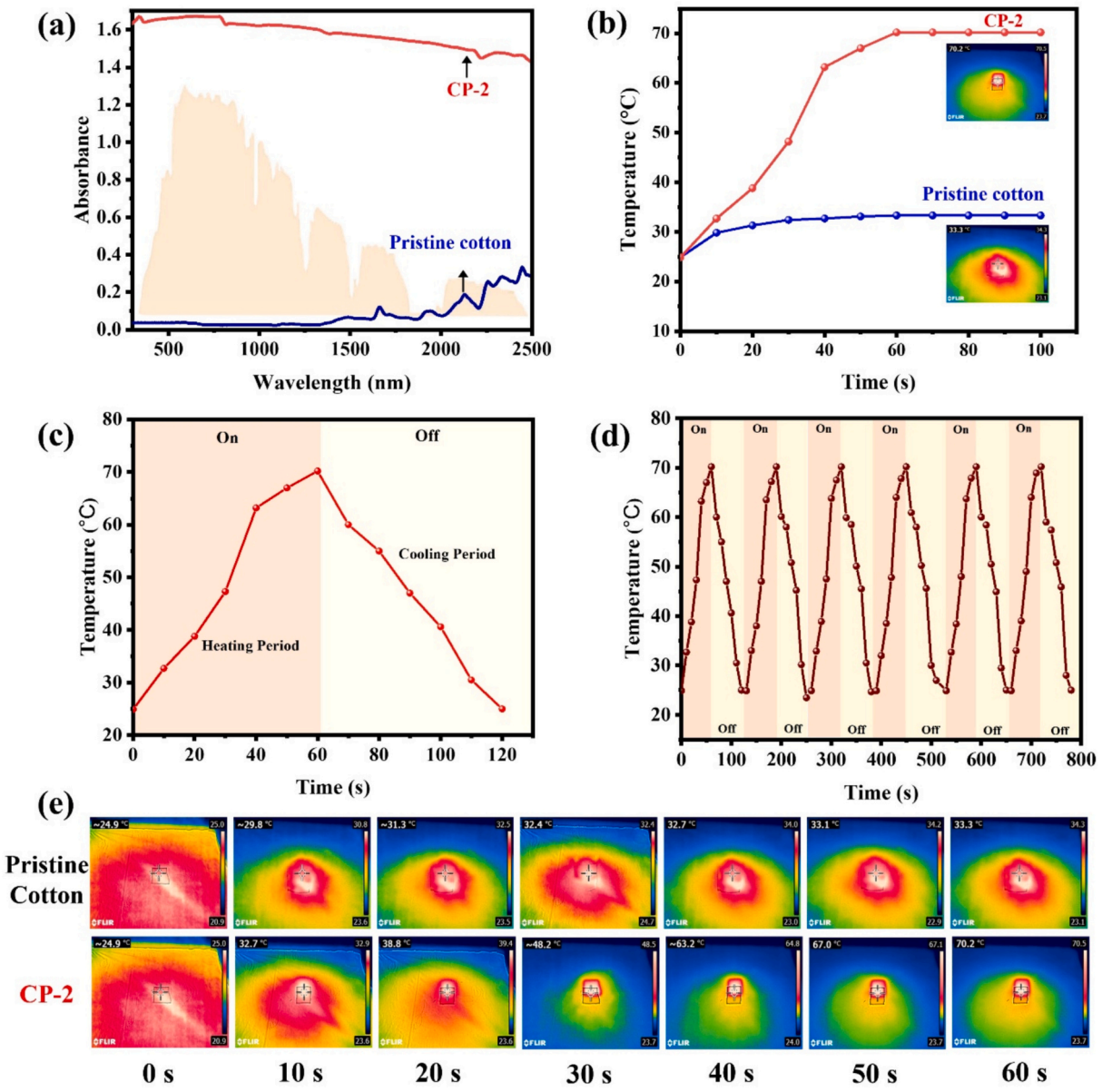

Fig. 6. (a) Standard solar spectrum and UV − Vis−NIR of absorption spectra in the range from 250 to 2500 nm of the pristine cotton and CP-2 sample. (b) Variation of surface temperature of the pristine and CP-2 sample under 1 kW/m^2 solar irradiation. The insets show infrared images under 1 kW/m^2 solar irradiation for 2 min. (c) Photothermal heating curve of CP-2 recorded during a light on-off cycle. (d) Variation of the surface temperature of CP-2 sample under series of on and off modes of light irradiation. (e) Infrared thermal images of pristine cotton and CP-2 sample throughout the exposure of xenon lamp illumination.

technologies [45], antimicrobial surfaces [46,47], oil remediation [48–50], and de-icing solutions [51,52]. Fig. 6b illustrates the comparative surface temperature profiles of pristine cotton and superhydrophobic CP-2 cotton fabric during exposure to xenon lamp irradiation. Under continuous illumination, the CP-2-coated cotton rapidly increases temperature up to 70.2 °C within 60 s, indicating a strong photothermal response. In contrast, the pristine cotton fabric showed negligible temperature (~ 40 °C) fluctuations throughout the exposure period, emphasizing the substantial enhancement in thermal performance provided by the CP-2 coating. Further analysis showed that CS/PDMS formulations demonstrated significant photothermal effects, which depended on the concentration of CS NPs in the coatings. As shown in Fig. 6c, the surface temperature increased rapidly with the light on and cooled quickly when it was turned off. The repeated photothermal effect, as shown in Fig. 6d, indicates that these fabrics retain their functional properties after multiple light exposure cycles, demonstrating durability and resilience. Such qualities are crucial for applications requiring consistent performance in varying environmental conditions, making these fabrics a promising choice for smart textiles and innovative technologies. Both the superhydrophobic characteristics and the intricate surface microstructure of the CP-2 sample remained intact even after undergoing multiple illumination cycles, as shown in Fig. 6d. Fig. 6e displays infrared thermal imaging, clearly highlighting the significant temperature variations between the pristine cotton and the CP-2 sample under xenon lamp illumination.

Further, the photothermal properties of the CP-2 sample were investigated with the surface contamination by dust particles. For a systematic analysis, one half of the CP-2 sample was deliberately covered with fine soil particles or small-sized stones, while the other half was kept bare, as illustrated in Fig. 7. Under illumination with light at an intensity of 1 kW/m^2, the surface temperature of the soil-contaminated CP-2 sample reached 59.9 °C, whereas the stone-contaminated part had a temperature of 64 °C. This noticeable difference in surface temperature can be attributed to the obstruction of light radiation, which

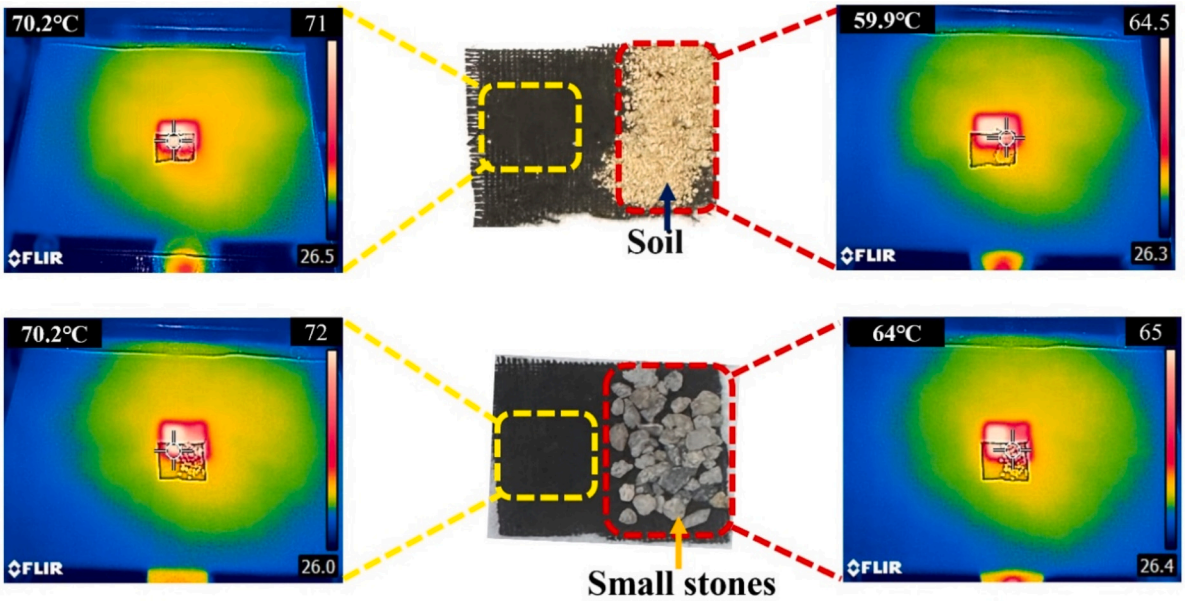

Fig. 7. Photothermal performance of CP-2 cotton fabric without or with coverage of soil and small stones.

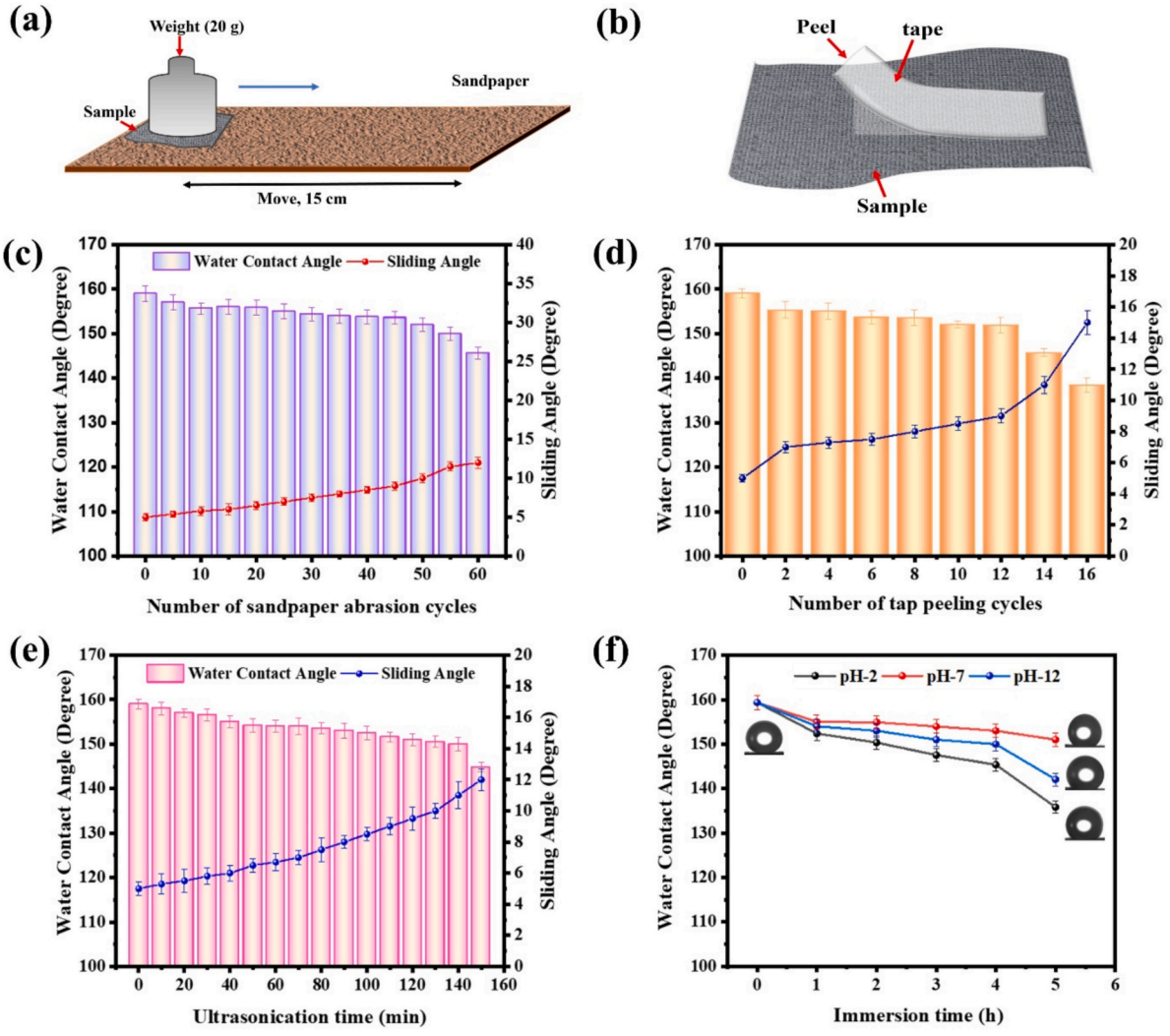

Fig. 8. Schematics of (a) sandpaper abrasion test and (b) adhesive tape test. The relationship between (c) WCA and sandpaper abrasion cycles, (d) WCA and adhesive tape peeling cycles, (e) WCA and ultrasonication time and (f) WCA and immersion time.

impeded the effective absorption of light energy. Despite the contaminants on the surface, these temperature levels are sufficient to deactivate microbes under light irradiation. This indicates that, the photothermal effect remains effective in achieving microbial deactivation even with dust. Furthermore, due to the unique superhydrophobic properties of the CP-2 sample, as water is poured over the surface, both the dust particles and the deactivated microbes can be effectively rinsed away. This investigation demonstrates the practical application of the coated fabric in environments where maintaining cleanliness and microbial control is crucial.

3.3. Mechanical stability

To evaluate the practical applicability of the as-prepared photothermal superhydrophobic cotton, it is crucial to examine its durability under various aggressive conditions [42,53]. The changes in mechanical properties of the cotton samples before and after the coating were monitored by measuring the tensile strength. The maximum load of the uncoated and coated samples were 14.42 N and 21.29 N, respectively. The corresponding maximum elongations in length were 25.92 mm and 32.25 mm, suggesting improved mechanical properties after the coating.

The coated cotton's stability was assessed by measuring the changes in WCA and SA following various stability tests. Fig. 8 illustrates the changes in WCA and SA after the cotton fabric was subjected to a series of rigorous evaluations: the sandpaper abrasion test, adhesive tape peeling test, and ultrasound treatment (simulates machine washing). Additionally, the fabric was immersed in alkaline and acidic solutions to investigate its chemical resilience. During the sandpaper abrasion test, the coated cotton was pasted on glass slide and was rubbed against sandpaper (grit no. 2000) under a controlled load in a linear motion at a consistent speed. This process can lead to the detachment of the coating material from the cotton surface, which may compromise the integrity of the surface structure. The coating loss is particularly significant as it directly affects the wettability characteristics of the cotton fabric [54]. Removing the coating materials diminishes the hydrophobic properties, leading to a decrease in WCA (Fig. 8c). The unique combination of CS and PDMS, along with PLA, enhances interlayer adhesion while maintaining superhydrophobicity through 55 abrasion cycles. Beyond this point, the WCA becomes 145.6°, and SA is 12°, showing minimal changes and indicating good durability against mechanical stress. The gradual decrease in WCA observed with an increasing number of sandpaper abrasion cycles can be attributed to the partial damage of the hierarchical micro/nanostructures [55]. As mechanical abrasion takes place, the embedded CS particles may become dislodged from the PDMS network, resulting in a smoother surface. This increases the actual contact area between the water and the substrate, which leads the surface to transition toward a hydrophobic state.

An adhesive tape was applied to the coated cotton surface, and a 200 g metal disc was rolled over it before peeling off the tape [39] (Fig. 8b). Fig. 8d shows that the WCA declines with the number of adhesive tape peeling cycles. Notably, the coating retains its superhydrophobic properties even after 12 peeling cycles, with a WCA of 151.8° and a SA of 9°. This suggests that liquids can easily move across the surface, indicating strong resistance to external adhesive components and ensuring durability despite mechanical stress. However, as the number of peeling cycles increases, the WCA drops below 140°. This significant decrease in WCA may be due to the detachment of the coating composite [56]. The detachment disrupts the hierarchical surface structure of the coating, resulting in a reduction in WCA.

The stability of washing processes is essential for cotton fabrics used in clothing. An ultrasound treatment was used to simulate washing conditions and assess stability by measuring changes in WCA and SA over varying durations, as shown in Fig. 8e [57]. The coated fabrics exhibited remarkable resilience, maintaining their superhydrophobic properties after 140 mins of continuous ultrasound treatment. Notably, extending the treatment to 140 min resulted in minor changes in WCA (150°) and SA (12°), indicating that the fabrics can withstand washing impacts well. Further, to investigate the washing resistance of coated cotton fabrics in harsh environments, we used a stirred washing method to mimic actual laundering conditions [58]. The washing solution was prepared by mixing 300 mL of tap water with 0.05 g of detergent in a 500 mL beaker. The coated cotton was added to the washing solution and the mixture was stirred at 150 RPM for various time intervals. After 15 min of stirring, the cotton was taken out and dried at 100 °C for 30 min to ensure complete drying. This process was repeated multiple times up to 150 min. The WCA was measured after every 15 min of washing. The WCA of CP-2 sample declined with washing time (Fig. S4). Notably, the coated cotton fabric demonstrated remarkable resilience, sustaining its superhydrophobic characteristics with a WCA of 152 ± 2° even after a 90 min of washing treatment. This finding highlights the effectiveness of the coating in preserving the fabric's hydrophobic properties under repeated laundering conditions, affirming its potential for practical applications. As the washing time increases to 150 min, the WCA decreases to below 130°. This reduction in WCA may be due to the detachment or degradation of the coating components, resulting in a diminished surface structure that negatively impacts the coating's wettability [59].

Clothing is often exposed to various chemical environments, including alkaline and acidic solutions, making it essential to evaluate the durability of fabric coatings. In a series of experiments, coated cotton fabric samples were immersed in solutions with pH levels of 2 (acidic), 7 (neutral), and 12 (alkaline) for 5 h. WCA were measured at one-hour intervals to assess hydrophobic properties. Results showed satisfactory performance across all pH levels. This indicates that while the coating retains some water repellence, it effectively withstands harsh chemical exposure, highlighting its real-world applicability. However, after 5 h, the WCA values began to decline, despite prolonged contact with different pH solutions (see Fig. 8f). Immersion in solutions with pH levels of 2, 7, and 12 over time resulted in a noticeable decrease in WCA [60]. This decline may be attributed to the chemical degradation or hydrolysis of functional groups, such as Si–O–Si or Si—C bonds, as well as changes in surface roughness. Both acidic and basic solutions can disrupt the siloxane network or leach out surface-modifying agents, which compromises the surface chemistry and morphology necessary for maintaining superhydrophobicity.

3.4. Flexibility, air permeability, water vapor transmission and breathability

The structural attributes of cotton fabrics, their weave pattern, fiber composition, and fragile nature are crucial in influencing their flexibility, breathability, and air permeability. It is collectively distributed to provide wearer comfort in daily applications. To evaluate the flexibility of both uncoated and coated (CP-2) samples, the fabric was naturally folded (Fig. 9a-b). A negligible variation in length was revealed. These results indicate that, the coating doesn't affect the flexibility of cotton.

The air permeability of the pristine cotton is 168 mm s^{-1}. Incorporating the PLA/CSNP/PDMS composite led to a slight reduction in the air permeability (102 mm s^{-1}). To study the air permeability, the coated sample was tied to the opening of a container with a rubber strip as shown in Fig. 9c and d. The container was filled with hot water. The results show that the water vapor was escaped from the coated sample after 10 s and condensed in the beaker as shown in Fig. 9(c, d) [61]. Furthermore, the breathability of the cotton was evaluated utilizing a chemical reaction containing ammonia and hydrochloric acid. Hydrochloric acid and ammonia solution were filled in two different containers [60]. As Fig. 9(e-f) depicts, no smoke was observed when the ammonia solution container cap was sealed and the HCl bottle was covered with pristine or coated cotton. However, when the cap of the ammonia solution container was removed, white smoke is produced due to the generation of ammonia chloride (NH_4Cl) (Fig. 9g, h). The intensity variation of the smoke suggests that the coating does not affect the air permeability significantly.

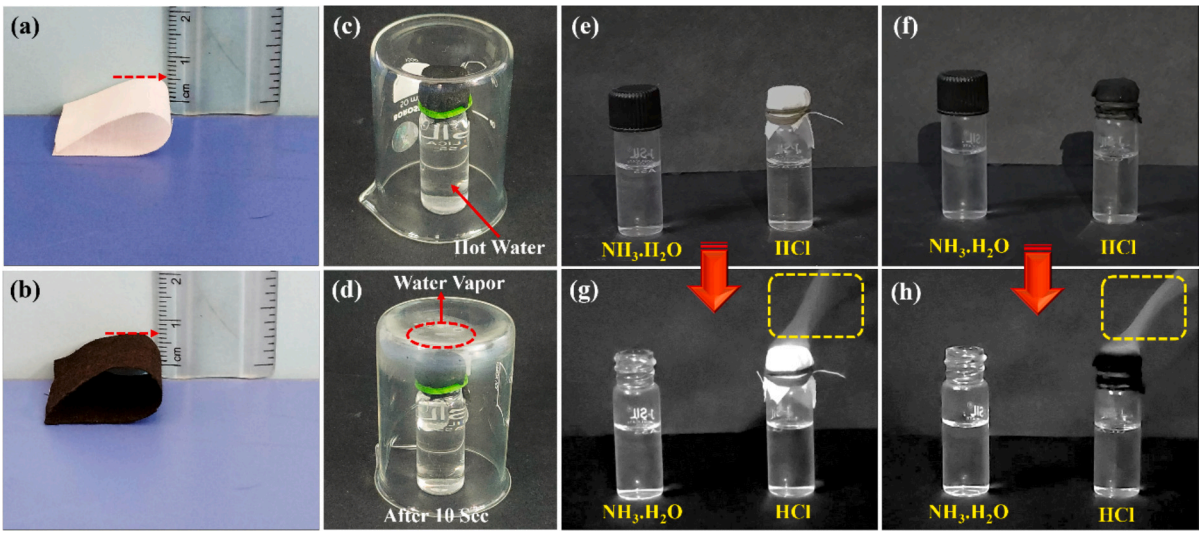

Fig. 9. Comparison of flexibility of (a) pristine, and (b) coated cotton fabric. (c, d) The photograph of CP-2 sample, showing water vapor condensed on roof of the beaker. (e-f) The breathability of the (e, g) pristine cotton and (f, h) CP-2 coated cotton fabric.

3.5. Self-cleaning performance

In outdoor environments, cotton materials often face significant contamination from various environmental pollutants such as dust, fine soil particles, and deactivating microbes. To evaluate the self-cleaning capabilities, experimental investigations were conducted where dust particles, specifically modelled by soil and chalk particles, were randomly distributed over the cotton samples. The testing setup involved adhering the sample first onto a glass slide using double-sided tape. These slides were then positioned at an angle of 6° within a petri dish. During the experiment, water droplets were deliberately introduced onto the surface of the dust-contaminated samples. With the pristine sample, the water droplets were rapidly absorbed by the adhering dust particles, which stuck to the cotton itself (Fig. 10 (a-c)). This behaviour can be attributed to the presence of hydroxyl groups on the surface of the pristine cotton, encouraging water to bind with the dust and the cotton fibers. In contrast, the CP-2 sample exhibited remarkable superhydrophobic properties, which conferred a significant self-cleaning ability. In this case, the water droplets formed spherical shapes and did not adhere to the surface; instead, they rolled off, effectively carrying the captured dust particles with them. The remarkable performance of CP-2 can be traced back to its intricate micro-nano surface structure created by the incorporation of CS NPs and the utilization of PDMS, which reduces surface energy. This dual-level architectural design facilitates the superhydrophobic effect and enhances the self-cleaning properties, as illustrated in Figs. 10 (d-f).

3.6. Self-sterilization performance

To evaluate the bacteria-repelling capabilities of the superhydrophobic surface derived from the CP-2 sample, the sample was strategically placed on the surface of an agar medium. As shown in Fig. 11, the superhydrophobic characteristics of the CP-2 surface significantly reduced the water/solid interfacial contact area, effectively minimizing bacterial adhesion. This property enables the surface to repel the majority of bacteria, highlighting its potential as a protective barrier against microbial colonization. In addition, the antibacterial efficacy of the coated fabric was rigorously assessed by exposing it to various durations of NIR laser irradiation at a wavelength of 700 nm. The model bacteria selected for this study were *Staphylococcus aureus*

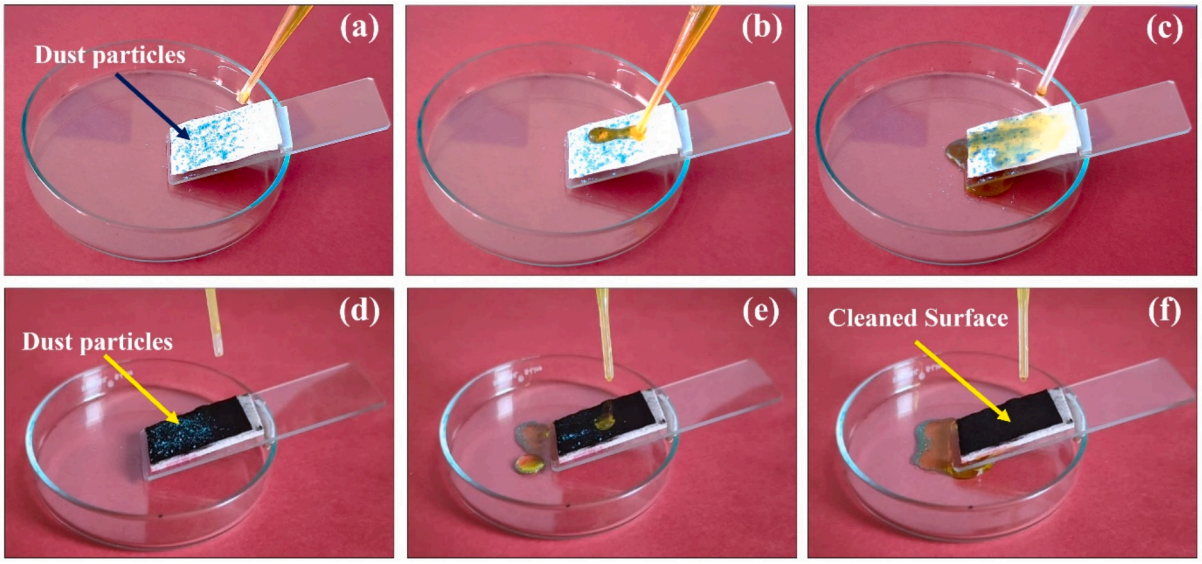

Fig. 10. Self-cleaning behaviour of (a-c) pristine cotton fabric, and (d-f) CP-2 sample against dust particles (contaminants appear like chalk powder).

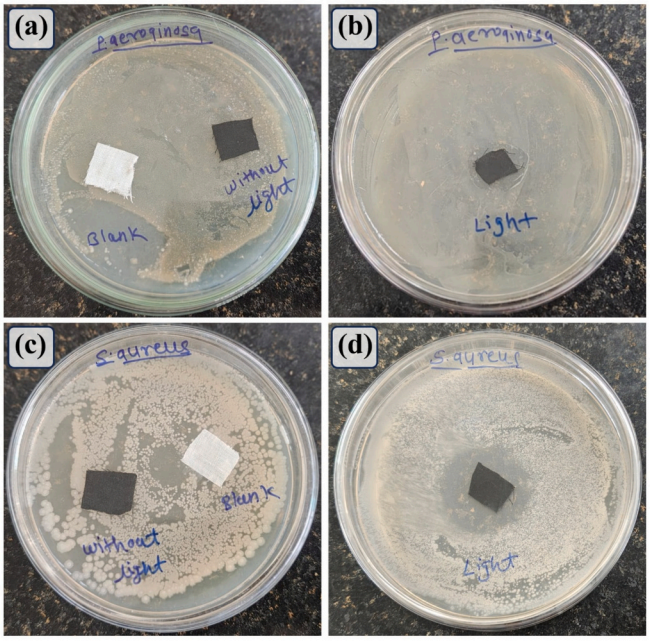

Fig. 11. Photothermal sterilization performance of pristine cotton and CP-2 samples against (a, b) *P. aeruginosa* and (c, d) *S. aureus* bacteria in (a, c) dark and (b, d) under NIR irradiation.

and *Pseudomonas aeruginosa*; both commonly associated with infections. After a 5 min exposure to the NIR laser, the bacterial survival rates on the CP-2 sample were significantly decreased, showing reductions of 45 % for *S. aureus* and 50 % for *P. aeruginosa* compared to untreated pristine cotton. When the duration of irradiation was increased to 10 min, the antibacterial performance improved further, resulting in survival rate reductions of 23 % for *S. aureus* and 18.4 % for *P. aeruginosa*.

These findings emphasize the remarkable antibacterial activity arising from the combined effects of the intrinsic superhydrophobic properties and the photothermal response induced by the laser irradiation. This synergy suggests that while the superhydrophobic surface effectively deters most bacterial adhesion, the few bacteria that do manage to adhere can be rapidly sterilized through photothermal therapy when exposed to NIR irradiation. Notably, the significant reduction in viable bacteria observed after 10 min of NIR irradiation underscores the surface's strong antibacterial potential, indicating its applicability in the developing self- sterilizing materials for various health-related applications.

4. Conclusions

The study reports a simple and efficient approach in developing a photothermal superhydrophobic cotton fabric. The fabrication involves applying sequential layers of polylactic acid (PLA) and a mixture of candle soot (CS) and polydimethylsiloxane (PDMS) using a cost-effective dip coating technique. The surface characterization revealed that the CS NPs are integrated within the PDMS network, resulting in a hierarchical rough structure that effectively traps an air layer on the surface, thereby reducing the water contact area. The designed formulation of PLA and CS/PDMS on the cotton fabric demonstrates superhydrophobicity, achieving a WCA of 159 ± 2° and a SA of 6°. The surface energy of the coated cotton fabric (4.7808 mN/m) was significantly lower than that of pristine cotton fabric (144 mN/m), contributing to its enhanced superhydrophobicity. The solid-liquid fraction of the coated cotton fabric was calculated to be 0.03015. Additionally, the presence of CS as a photothermal component in the coating generates heat when exposed to NIR light through the photothermal effect, reaching temperatures of up to 70.2 °C within 60 s under 1 sun illumination. The deactivation of *S. aureus* and *P. aeruginosa* bacteria under light illumination confirms that the composite coating exhibits excellent self-sterilization properties. Furthermore, results regarding mechanical stability indicate that the coating maintains its superhydrophobicity after withstanding 55 cycles of sand abrasion, 12 cycles of adhesive tape peeling, 140 min of ultrasound and 90 min of washing treatment. Furthermore, the coated cotton fabric demonstrated a good response in terms of flexibility, breathability, air permeability, and water vapor transmission. These results prove the high potential of the developed superhydrophobic cotton fabric in developing contactless microbial sterilization and self-cleaning technologies.

CRediT authorship contribution statement

Rutuja A. Ekunde: Writing – original draft, Methodology, Investigation, Conceptualization. **Rajaram S. Sutar:** Writing – original draft, Methodology, Investigation, Conceptualization. **Sagar S. Ingole:** Methodology, Investigation. **Akshay R. Jundle:** Methodology, Investigation. **Pradip P. Gaikwad:** Methodology, Investigation. **Viswanathan S. Saji:** Writing – review & editing, Validation. **Shanhu Liu:** Writing – review & editing, Validation. **Appasaheb K. Bhosale:** Writing – review & editing, Supervision, Conceptualization. **Sanjay S. Latthe:** Writing – review & editing, Supervision, Project administration, Funding acquisition, Conceptualization.

Declaration of competing interest

The authors declare that they have no known competing financial interests or personal relationships that could have appeared to influence the work reported in this paper.

Acknowledgements

One of the authors, SSL is grateful for financial assistance received through Seed Money Scheme from Vivekanand College, Kolhapur (Empowered Autonomous), Ref. No. VCK/3108/2023-24 dated 30/03/2024. The authors gratefully acknowledge the Department of Physics, Savitribai Phule Pune University, for providing access to the Scanning Electron Microscope facility, which was established with financial support from the Department of Science and Technology (DST), Government of India, under the DST-FIST Programme (SR/FST/PS II-003/2000).

Appendix A. Supplementary data

Supplementary data to this article can be found online at https://doi.org/10.1016/j.porgcoat.2025.109514.

Data availability

Data will be made available on request.

References

[1] J.J. Bartoszko, M.A.M. Farooqi, W. Alhazzani, M. Loeb, Medical masks vs N95 respirators for preventing COVID-19 in healthcare workers: a systematic review and meta-analysis of randomized trials, Influenza Other Respir. Viruses 14 (2020) 365–373.
[2] A. Konda, A. Prakash, G.A. Moss, M. Schmoldt, G.D. Grant, S. Guha, Aerosol filtration efficiency of common fabrics used in respiratory cloth masks, ACS Nano 14 (2020) 6339–6347.
[3] S. Kumar, M. Karmacharya, S.R. Joshi, O. Gulenko, J. Park, G.-H. Kim, Y.-K. Cho, Photoactive antiviral face mask with self-sterilization and reusability, Nano Lett. 21 (2020) 337–343.
[4] W.H. Organization, Advice on the Use of Masks in the Context of COVID-19: Interim Guidance, 6 April 2020, in: Advice on the Use of Masks in the Context of COVID-19: Interim Guidance, 6 April 2020, 2020.
[5] A. SadrHaghighi, R. Sarvari, E. Fakhri, V. Poortahmasebi, N. Sedighnia, M. Torabi, M. Mohammadzadeh, A.H. Azhiri, M. Eskandarinezhad, K. Moharamzadeh,

Copper-nanoparticle-coated melt-blown facemask filter with antibacterial and SARS-CoV-2 antiviral ability, ACS Appl. Nano Mater. 6 (2023) 12849–12861.
[6] N.H. Leung, D.K. Chu, E.Y. Shiu, K.-H. Chan, J.J. McDevitt, B.J. Hau, H.-L. Yen, Y. Li, D.K. Ip, J.M. Peiris, Respiratory virus shedding in exhaled breath and efficacy of face masks, Nat. Med. 26 (2020) 676–680.
[7] H. Zhong, Z. Zhu, P. You, J. Lin, C.F. Cheung, V.L. Lu, F. Yan, C.-Y. Chan, G. Li, Plasmonic and superhydrophobic self-decontaminating N95 respirators, ACS Nano 14 (2020) 8846–8854.
[8] E. Oral, K.K. Wannomae, R. Connolly, J. Gardecki, H.M. Leung, O. Muratoglu, A. Griffiths, A.N. Honko, L.E. Avena, L.G. McKay, Vapor H2O2 sterilization as a decontamination method for the reuse of N95 respirators in the COVID-19 emergency, MedRxiv (2020) 2020–2024, 2020.2004.2011.20062026.
[9] S.A. Grinshpun, M. Yermakov, M. Khodoun, Autoclave sterilization and ethanol treatment of re-used surgical masks and N95 respirators during COVID-19: impact on their performance and integrity, J. Hosp. Infect. 105 (2020) 608–614.
[10] N. Celik, F. Sahin, S.S. Ozel, G. Sezer, N. Gunaltay, M. Ruzi, M.S. Onses, Self-healing of biocompatible superhydrophobic coatings: the interplay of the size and loading of particles, Langmuir 39 (2023) 3194–3203.
[11] R. Soni, S.R. Joshi, M. Karmacharya, H. Min, S.-K. Kim, S. Kumar, G.-H. Kim, Y.-K. Cho, C.Y. Lee, Superhydrophobic and self-sterilizing surgical masks spray-coated with carbon nanotubes, ACS Appl. Nano Mater. 4 (2021) 8491–8499.
[12] P. Kumar, S. Roy, A. Sarkar, A. Jaiswal, Reusable MoS2-modified antibacterial fabrics with photothermal disinfection properties for repurposing of personal protective masks, ACS Appl. Mater. Interfaces 13 (2021) 12912–12927.
[13] X. Su, H. Li, X. Lai, Z. Yang, Z. Chen, W. Wu, X. Zeng, Vacuum-assisted layer-by-layer superhydrophobic carbon nanotube films with electrothermal and photothermal effects for deicing and controllable manipulation, J. Mater. Chem. A 6 (2018) 16910–16919.
[14] E. Pakdel, J. Sharp, S. Kashi, W. Bai, M.P. Gashti, X. Wang, Antibacterial superhydrophobic cotton fabric with photothermal, self-cleaning, and ultraviolet protection functionalities, ACS Appl. Mater. Interfaces 15 (2023) 34031–34043.
[15] H. Zhong, Z. Zhu, J. Lin, C.F. Cheung, V.L. Lu, F. Yan, C.-Y. Chan, G. Li, Reusable and recyclable graphene masks with outstanding superhydrophobic and photothermal performances, ACS Nano 14 (2020) 6213–6221.
[16] A. Duan, F. Gu, X. Jiang, J. Du, D. Shao, C. Xu, Washable superhydrophobic cotton fabric with photothermal self-healing performance based on nanocrystal-MXene, ACS Appl. Mater. Interfaces 17 (2025) 9923–9936.
[17] N. Arshad, M.S. Irshad, M. Alomar, J. Guo, M.S. Asghar, N. Mushtaq, M. Yousaf, U. Ghazanfar, M. Shah, X. Wang, Exploring perovskite oxide for advancing salt-resistant photothermal membranes and reliable thermoelectric generators, Chem. Eng. J. 475 (2023) 146200.
[18] R. Iqbal, B. Majhy, A. Sen, Facile fabrication and characterization of a PDMS-derived candle soot coated stable biocompatible superhydrophobic and superhemophobic surface, ACS Appl. Mater. Interfaces 9 (2017) 31170–31180.
[19] S. Hao, H. Han, Z. Yang, M. Chen, Y. Jiang, G. Lu, L. Dong, H. Wen, H. Li, J. Liu, Recent advancements on photothermal conversion and antibacterial applications over MXenes-based materials, Nano-Micro Lett. 14 (2022) 178.
[20] J. Chen, Q. Huang, H. Huang, L. Mao, M. Liu, X. Zhang, Y. Wei, Recent progress and advances in the environmental applications of MXene related materials, Nanoscale 12 (2020) 3574–3592.
[21] Y. Lin, K. Lu, H. Zhang, Y. Zou, H. Chen, Y. Zhang, Q. Yu, Multifunctional coatings based on candle soot with photothermal bactericidal property and desired biofunctionality, J. Colloid Interface Sci. 649 (2023) 986–995.
[22] Y. Lin, H. Zhang, Y. Zou, K. Lu, L. Li, Y. Wu, J. Cheng, Y. Zhang, H. Chen, Q. Yu, Superhydrophobic photothermal coatings based on candle soot for prevention of biofilm formation, J. Mater. Sci. Technol. 132 (2023) 18–26.
[23] S. Wu, Y. Du, Y. Alsaid, D. Wu, M. Hua, Y. Yan, B. Yao, Y. Ma, X. Zhu, X. He, Superhydrophobic photothermal icephobic surfaces based on candle soot, Proc. Natl. Acad. Sci. 117 (2020) 11240–11246.
[24] X. Su, H. Li, X. Lai, L. Zhang, J. Wang, X. Liao, X. Zeng, Vapor–liquid sol–gel approach to fabricating highly durable and robust superhydrophobic polydimethylsiloxane@ silica surface on polyester textile for oil–water separation, ACS Appl. Mater. Interfaces 9 (2017) 28089–28099.
[25] G. Zheng, Y. Cui, Z. Jiang, M. Zhou, Y. Yu, P. Wang, Q. Wang, Superhydrophobic, photothermal, and UV-resistant coatings obtained by polydimethylsiloxane treating self-healing hydrophobic chitosan-tannic acid surface for oil/water separation, Chem. Eng. J. 473 (2023) 145258.
[26] S. Chen, H. Li, X. Lai, S. Zhang, X. Zeng, Superhydrophobic and phosphorus-nitrogen flame-retardant cotton fabric, Prog. Org. Coat. 159 (2021) 106446.
[27] Y. Guan, B. Bi, D. Qiao, S. Cao, W. Zhang, Z. Wang, H. Zeng, Y. Li, Bioinspired superhydrophobic polylactic acid aerogel with a tree branch structure for the removal of viscous oil spills assisted by solar energy, J. Mater. Chem. A 12 (2024) 9850–9862.
[28] L. Jiang, X. Zhu, J. Li, J. Shao, Y. Zhang, J. Zhu, S. Li, L. Zheng, X.-P. Li, S. Zhang, Electroactive and breathable protective membranes by surface engineering of dielectric nanohybrids at poly (lactic acid) nanofibers with excellent self-sterilization and photothermal properties, Sep. Purif. Technol. 339 (2024) 126708.
[29] W. Sun, K. Lv, Y. Lou, D. Zeng, X. Lin, Highly durable superhydrophobic surfaces based on a protective frame and crosslinked PDMS-candle soot coatings, Mater. Res. Exp. 9 (2022) 096401.
[30] K. Yan, J. Wang, Y. Zong, Q. Xu, A multifunctional coating toward wearable superhydrophobic fabric sensor with self-healing and flame-retardant properties with high fire alarm response, Chem. Eng. J. 489 (2024) 151315.
[31] D. Saini, J. Gunture, J. Kaushik, R. Aggarwal, K.M. Tripathi, S.K. Sonkar, Carbon nanomaterials derived from black carbon soot: a review of materials and applications, ACS Appl. Nano Mater. 4 (2021) 12825–12844.
[32] X. Wei, J. Wei, Y. Feng, J. Wang, Photothermal hydrophobic coating with light-trapping and thermal isolated effects for efficient photothermal anti-icing/de-icing, Prog. Org. Coat. 179 (2023) 107550.
[33] Z. Wu, K. Fang, W. Chen, Y. Zhao, Y. Xu, C. Zhang, Durable superhydrophobic and photocatalytic cotton modified by PDMS with TiO2 supported bamboo charcoal nanocomposites, Ind. Crop. Prod. 171 (2021) 113896.
[34] R.S. Sutar, B. Shi, S.S. Kanchankoti, S.S. Ingole, W.S. Jamadar, A.J. Sayyad, P. B. Khot, K.K. Sadasivuni, S.S. Latthe, S. Liu, Development of self-cleaning superhydrophobic cotton fabric through silica/PDMS composite coating, Surf. Topogr. Metrol. Prop. 11 (2023) 045004.
[35] S.M. Mirvakili, I.W. Hunter, Multidirectional artificial muscles from nylon, in: Google Patents, 2021.
[36] M. Zhang, C. Guo, Y. Wang, Y. Zhang, H. Wu, L. Huang, Y. Ni, C. Ding, L. Chen, NIR-responsive collagen-based sponge coated with polydimethylsiloxane/candle soot for oil-water separation, Pap. Biomater. 7 (2022) 30–41.
[37] B. Zhang, J. Duan, Y. Huang, B. Hou, Double layered superhydrophobic PDMS-Candle soot coating with durable corrosion resistance and thermal-mechanical robustness, J. Mater. Sci. Technol. 71 (2021) 1–11.
[38] C. Thamaraiselvan, E. Manderfeld, M.N. Kleinberg, A. Rosenhahn, C.J. Arnusch, Superhydrophobic candle soot as a low fouling stable coating on water treatment membrane feed spacers, ACS Appl. Bio Mater. 4 (2021) 4191–4200.
[39] C. Qian, L. Wang, Q. Li, X. Chen, A strategy of candle soot-based photothermal icephobic superhydrophobic surface, Coatings 14 (2024) 612.
[40] T.A. Ekunde, P.P. Gaikwad, R.S. Sutar, S.S. Kshirsagar, R.A. Ekunde, A.M. Yelpale, X. Huang, V.S. Saji, S. Liu, S.S. Latthe, Superhydrophobic northern tooth-like ZnO nanosheets on stainless steel mesh for oil-water separation, J. Water Process Eng. 71 (2025) 107368.
[41] A.P. Rananavare, R. Jain, J. Lee, Recent developments in superhydrophobic textiles: a status review, J. Coat. Technol. Res. 22 (2024) 1.
[42] Q. Xue, J. Wu, Z. Lv, Y. Lei, X. Liu, Y. Huang, Photothermal superhydrophobic chitosan-based cotton fabric for rapid deicing and oil/water separation, Langmuir 39 (2023) 9912–9923.
[43] R.S. Sutar, S.S. Latthe, X. Wu, K. Nakata, R. Xing, S. Liu, A. Fujishima, Design and mechanism of photothermal soft actuators and their applications, J. Mater. Chem. A 12 (2024) 17896–17922.
[44] T. Xu, S. Zhang, S. Han, Y. Qin, C. Liu, M. Xi, X. Yu, N. Li, Z. Wang, Fast solar-to-thermal conversion/storage nanofibers for thermoregulation, stain-resistant, and breathable fabrics, Ind. Eng. Chem. Res. 60 (2021) 5869–5878.
[45] L. Yu, P. Si, L. Bauman, B. Zhao, Synergetic combination of interfacial engineering and shape-changing modulation for biomimetic soft robotic devices, Langmuir 36 (2020) 3279–3291.
[46] L.-H. Zhang, J.-L. Yang, Y.-Y. Song, Y. Liu, Z.-Q. Zhang, Synergistic antibacterial surface with liquid repellency and enhanced photothermal bactericidal activity, Langmuir 39 (2023) 8379–8389.
[47] S. Liu, J. Zheng, L. Hao, Y. Yegin, M. Bae, B. Ulugun, T.M. Taylor, E.A. Scholar, L. Cisneros-Zevallos, J.K. Oh, Dual-functional, superhydrophobic coatings with bacterial anticontact and antimicrobial characteristics, ACS Appl. Mater. Interfaces 12 (2020) 21311–21321.
[48] Y. Liu, S. Cheng, S.K. Kannan, P. Zhang, R.S. Sutar, B. Shi, S. Liu, Scalable superhydrophobic CB/PVFM sponge for enhanced cleanup of crude oil exploiting photothermal and electrothermal effects, ACS Appl. Polym. Mater. 6 (2024) 8367–8376.
[49] H.-T. Ren, C.-C. Cai, W.-B. Cao, D.-S. Li, T.-T. Li, C.-W. Lou, J.-H. Lin, Superhydrophobic TiN-coated cotton fabrics with nanoscale roughness and photothermal self-healing properties for effective oil–water separation, ACS Appl. Nano Mater. 6 (2023) 11925–11933.
[50] Z. Wu, K. Zheng, Z. Cheng, S. Zhou, Solar-assisted superhydrophobic MoS2/PDMS/MS sponge for the efficient cleanup of viscous oil, Langmuir 38 (2022) 10902–10914.
[51] Z. Xie, H. Wang, Q. Deng, Y. Tian, Y. Shao, R. Chen, X. Zhu, Q. Liao, Heat transfer characteristics of carbon-based photothermal superhydrophobic materials with thermal insulation micropores during anti-icing/deicing, J. Phys. Chem. Lett. 13 (2022) 10237–10244.
[52] J. Wei, X. Wei, M. Hou, J. Wang, Fluorine-free photothermal superhydrophobic copper oxide micro-/nanostructured coatings for anti-icing/de-icing applications, ACS Appl. Nano Mater. 6 (2023) 9928–9938.
[53] H.-B. Yuan, M. Zhao, X. Zhu, D. Sha, G. Chen, T. Xing, Facile fabrication of durable and breathable superhydrophobic cotton fabric for self-cleaning, UV-blocking, anti-icing, and photothermal de-icing, Cellulose 31 (2024) 4627–4644.
[54] X.-J. Guo, D. Zhang, C.-H. Xue, B.-Y. Liu, M.-C. Huang, H.-D. Wang, X. Wang, F.-Q. Deng, Y.-P. Pu, Q.-F. An, Scalable and mechanically durable superhydrophobic coating of SiO2/polydimethylsiloxane/epoxy nanocomposite, ACS Appl. Mater. Interfaces 15 (2023) 4612–4622.
[55] R.S. Sutar, S.S. Latthe, A. Sargar, C. Patil, V. Jadhav, A. Patil, K. Kokate, A. K. Bhosale, K.K. Sadasivuni, S.V. Mohite, Spray deposition of PDMS/candle soot NPs composite for self-cleaning superhydrophobic coating, in: Macromol. Symp., Wiley Online Library, 2020, p. 2000031.
[56] G. Chen, Y. Zhang, K. Zhang, W. Lv, Z. Lv, X. Gao, Y. Huang, Photothermal superhydrophobic zinc oxide cotton fabric based on an impregnation method, Langmuir 41 (2025) 9857–9868.
[57] Q. Shang, C. Liu, J. Chen, X. Yang, Y. Hu, L. Hu, Y. Zhou, X. Ren, Sustainable and robust superhydrophobic cotton fabrics coated with castor oil-based nanocomposites for effective oil–water separation, ACS Sustain. Chem. Eng. 8 (2020) 7423–7435.

[58] H. Ou, Z. Dai, Y. Gao, B. Zhou, Breathable fabrics with robust superhydrophobicity via in situ formation of hierarchical surface morphologies, ACS Appl. Mater. Interfaces 15 (2023) 39989–40000.
[59] J. Chen, L. Yuan, C. Shi, C. Wu, Z. Long, H. Qiao, K. Wang, Q.H. Fan, Nature-inspired hierarchical protrusion structure construction for washable and wear-resistant superhydrophobic textiles with self-cleaning ability, ACS Appl. Mater. Interfaces 13 (2021) 18142–18151.
[60] R.S. Sutar, S.G. Kodag, R.A. Ekunde, A.S. Sawant, T.A. Ekunde, S. Nagappan, Y. H. Kim, V.S. Saji, S. Liu, S.S. Latthe, Durable self-cleaning superhydrophobic cotton fabrics for wearable textiles, Ind. Crop. Prod. 222 (2024) 119717.
[61] E. Li, Y. Pan, C. Wang, C. Liu, C. Shen, C. Pan, X. Liu, Asymmetric superhydrophobic textiles for electromagnetic interference shielding, photothermal conversion, and solar water evaporation, ACS Appl. Mater. Interfaces 13 (2021) 28996–29007.